

Dosimetric Study in Tomotherapy Based on AAPM TG 119 Structures: A Longitudinal Moving Phantom Case

Nuruddin Nasution^{1,2}, Wahyu Edy Wibowo², Adi Teguh Purnomo³, Supriyanto Ardjo Pawiro^{1,*}

1. Department of Physics, Faculty of Mathematics and Natural Sciences, Universitas Indonesia, Depok, West Java, 16424, Indonesia
2. Department of Radiotherapy, Cipto Mangunkusumo General Hospital, Jakarta, 10430, Indonesia
3. Transmedik Indonesia, Jakarta, 10410, Indonesia

ARTICLE INFO	ABSTRACT
<p>Article type: Original Paper</p> <hr/> <p>Article history: Received: Apr 08, 2020 Accepted: Aug 06, 2020</p> <hr/> <p>Keywords: Tomotherapy Intensity Modulated Radiotherapy Dosimetric Impact</p>	<p>Introduction: Tomotherapy beam delivery is in the helical form. Therefore, the dose distribution will be more complex while target is moving. In this study, we sought to evaluate the dosimetric impact due to longitudinal motion in the phantom of a tomotherapy machine.</p> <p>Material and Methods: Cheese and Delta⁴ phantom[†] were placed on a respiratory motion platform. They moved in longitudinal directions at the amplitudes of 2, 4, 6, 8, and 10 mm. The period of that movement was 4 and 6 s with the field widths of 25 and 50 mm, respectively. The C-shaped complex target was modified according to the American Association of Physicists in Medicine (AAPM) Task Group (TG) 119. The planning verifications were evaluated through point dose, gamma index value, and dose-volume histogram (DVH).</p> <p>Results: Discrepancy of the dose measurements ranged from -1.254 to -14.421%. The range of gamma index value was 61.2 ± 1.23% to 100 ± 0.00. The DVH evaluation showed that the homogeneity index (HI) and the minimum dose to receive by 95% (D_{95%}) of the target structure were 0.247 to 0.389 and -0.061 to -0.271 Gy, respectively. The maximum dose (D_{Max}) of the organ at risk (OAR) structure was 0.082 to 0.327 Gy.</p> <p>Conclusion: The motion could induce dose discrepancies in tomotherapy dose distribution. The selection of the jaw field width in tomotherapy is crucial for intensity-modulated radiotherapy (IMRT) techniques with moving targets. For larger field widths, the dose discrepancy between the planned and measured doses exhibited an excellent result for gamma index and dose coverage.</p>

► Please cite this article as:

Nasution N, Wibowo WE, Purnomo AT, Pawiro SA. Dosimetric Study in Tomotherapy Based on AAPM TG 119 Structures: A Longitudinal Moving Phantom Case. *Iran J Med Phys* 2021; 18: 331-338. 10.22038/ijmp.2020.47698.1762.

Introduction

Beam delivery in tomotherapy is in the helical form as a result of the combination of longitudinal direction table with constant speed. During irradiation, gantry is rotated and multi-leaf collimator (MLC) moves simultaneously [1]. As the shape of the tumor becomes more sophisticated, internal organ motion becomes an issue with increased attention to the development of radiotherapy techniques, such as intensity-modulated radiotherapy (IMRT) and image-guided radiotherapy (IGRT) [2].

American Association of Physicists in Medicine (AAPM) Task Group (TG) 119 has published a guideline to conduct IMRT commissioning tests with different levels of target complexity [3]. TG-119 recommended planning tests, treatment delivery, and dose measurement. It consists of two preliminary tests and five test cases of IMRT with an increased level of complexity. The tests were performed using a ionization chamber, film, and 2D arrays to assess the accuracy of the planning system and treatment delivery. Based on this document, C-shape cases were

chosen to represent the target shape complexity in IMRT case.

Internal organ movement during irradiation can result in the potential variation of dose distribution between the planned dose and the dose delivered [4]. Several studies on internal organ motion have reported that superior-inferior organ motion is more dominant than other motion directions [5, 6]. In the case of a moving target, it would make artifacts towards the distribution of the tomotherapy dose. Such artifacts have been identified as dose rounding, that is, penumbra broadening at the edge of target volume along the direction of tumor's motion [7, 8], dose rippling for non-synchronized table motion and the target's internal motion [8-10], and the effect of the non-synchronization of MLC opening charged by target complexity with the target's internal motion [7].

Several publications have studied motion effects in tomotherapy using a moving phantom. Klein et al. [11] analyzed the gamma index and dose longitudinal profile in a moving target with a simple target shape varying its motion amplitude and periods. Park et al.

*Corresponding Author: Tel: (+62-21) 787 2610, Fax: (+62-21) 7863441; supriyanto.p@sci.ui.ac.id

[12] reported the analysis of gamma index towards the effect of target motion by inserting internal target volume (ITV) parameters. Kim et al. [13] also analyzed an artifact on a longitudinal dose caused by target motion, where the target was delineated in simple and complex shapes. Nevertheless, the target shape delineation and the dose objective of the planning did not follow the standard protocol outlined in the AAPM TG 119 report as an implementation of the IMRT commissioning test [3].

In the present work, we evaluated the dosimetric impact of longitudinal motion of the target by comparing the variation of dose distribution between the planned and measured doses in a moving phantom using the parameters of amplitude and period. In this study, the Virtual water™ phantom (normally called "Cheese" phantom) (Tomotherapy Inc., USA) was employed, which is used as a standard phantom in quality assurance measurements for the tomotherapy device [14]. Additionally, the AAPM TG 119 report was used as a protocol to delineate the target and other planning dose objectives.

Materials and Methods

Delta⁴ phantom⁺ (ScandiDos AB., Upsalla, Sweden) and Cheese phantom with homogeneous densities were employed in this work. The CIRS dynamic phantom platform model 008 PL (CIRS Inc., Norfolk, VA, USA) and CIRS motion control software version 2.1.2 were used during irradiation to simulate the motion effect and control the movement of the phantom in the superior-inferior direction with the variation of amplitude and period. Delta⁴ phantom⁺, was made of Poly Methyl Methacrylate (PMMA), works with two arranged orthogonal diodes attached to a PMMA cylinder to measure and compare the composite dose distribution generated from the helical tomotherapy machine (Tomotherapy, Inc., Wisconsin, USA). The Delta⁴ Phantom⁺ diameter is 220 mm, and its density is 1.19

g/cc with a relative electron density of 1.147 g/cc. A total of 1069 cylindrical p-type silicon diodes, each with an active area of 0.78 mm², are placed arthogonally in an area of 200 × 200 mm² [15]. Cheese phantom is a cylinder-shaped homogeneous phantom made of a material with a density of 1.047 g/cc. It is 30 cm in diameter and 18 cm in thickness. This phantom is used to measure a point dose using Exradin A1SL ionization chamber detector with a 0.053-cc collecting volume, and its collecting outer volume diameter is 4 mm (Standard Imaging, Middleton, WI).

In the treatment planning system (TPS) version 5.1.2.12 (Tomotherapy, Inc., Wisconsin, USA), computed tomography (CT) image dataset of Cheese phantom was generated using CT-simulator GE Bright Speed device (GE Healthcare, Inc., WI, USA), whereas the Delta⁴ phantom⁺ used virtual CT-image dataset provided by ScandiDos AB. Contours of the structure were delineated in the tomotherapy treatment planning system, which consisted of OARs, target, and active volume of the A1SL detector, as seen in Figure 1. The active volume of A1SL detector was delineated based on the outer boundary of the detector cavity and compared it to the detector specifications. These structures were delineated to obtain the average dose of planning results used as a comparison between the measured point dose and the planned dose. Following AAPM TG-119 report, the original target was delineated in a C-shaped contour surrounding the original OAR structure with the lengths of 8 cm and 10 cm for the original target and OAR structure, respectively. An additional margin was expanded from the original C-shaped target contour in a superior-inferior target to account for the motion amplitude variation set during the measurement. The motion amplitude variation in the superior-inferior direction was set at 2, 4, 6, 8, and 10 mm, such that the margin-expanded contours were also delineated at 2, 4, 6, 8, and 10 mm from the original target contour.

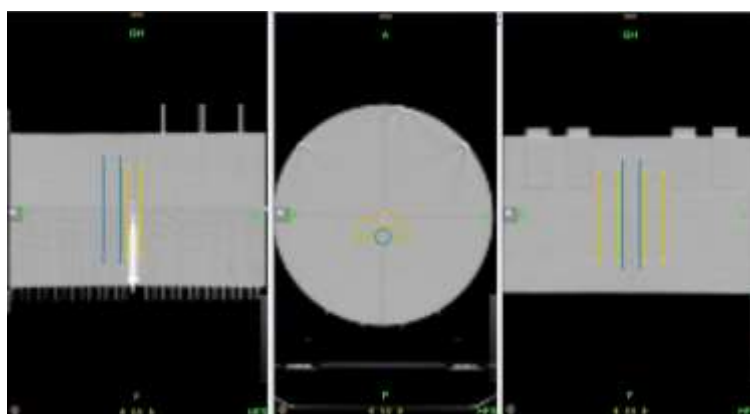


Figure 1. Sagittal (left), transversal (center), and coronal (right) CT images of the body phantom with the contours of target volume C-shaped (yellow) and OAR (blue) according to AAPM TG-119.

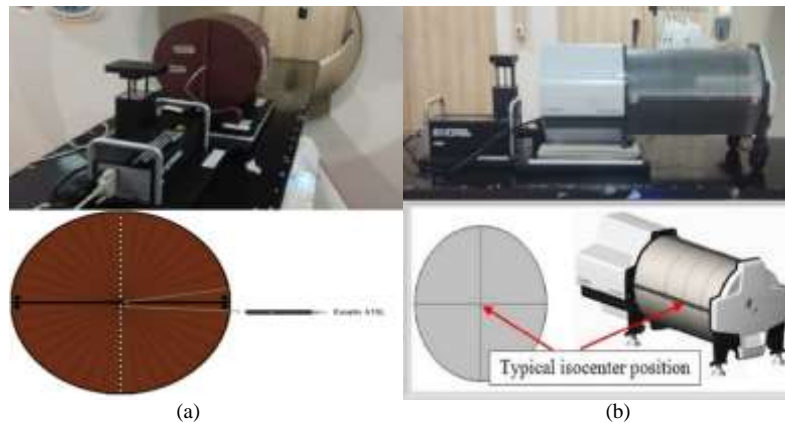


Figure 2. The set up of measurement a. point dose with Cheese phantom, and b. index gamma and DVH with Delta⁴ phantom⁺.

The planning was created in the CT Image dataset of the Cheese phantom and calculated in TomoPlan TPS with the dose prescriptions of 50 Gy delivered in 25 fractions. To obtain the planning objectives, the field widths of 25 mm and 50 mm were employed in the calculation process, except for 10 mm as the smallest field width that is no longer used clinically to treat a moving target. The planning parameters, such as pitch and modulation factor (MF), were varied to generate the same planning objectives for each field width used. The target should not receive less than 50 Gy within 95% volume or more than 55 Gy received in 10% volume. Moreover, the OAR structure must not have more than 25 Gy in 5% volume [3].

The planning result of the Cheese phantom was opened and recalculated in the delivery quality assurance (DQA) station to generate quality assurance (QA) planning using Delta⁴ phantom⁺. Then, radiotherapy (RT) dose, RT plan, and RT structure were exported from TomoPlan and imported to ScandiDos software version August 2017 release, as reference data for the dose comparison between the planned and measured doses. As a result, gamma index analysis and dose-volume histogram DVH comparison could be displayed automatically in the ScandiDos immediately after the measurement. The ScandiDos software could generate the DVH information from the measured dose provided that the RT structure from the planning image is imported into the software. Additionally, DVH comparison between the planned and measured DVH can be performed.

Cheese phantom, for point dose measurement, was placed on the tomotherapy couch with the small ion chamber holes facing against the gantry and aligned with the virtual isocenter. The A1SL detector was located vertically at 5 mm below the midline of the Cheese phantom. Furthermore, the Delta⁴ phantom⁺ was aligned with the virtual isocenter as seen in Figure 2. Prior to the measurement, mega voltage computed tomography (MVCT) images were taken for each phantom for phantom position verification, and the irradiation was delivered with the phantom setup varied with amplitudes and period. For both point dose and gamma index measurements were repeated three times

to reduce the uncertainty between the time when the phantom starts moving and the irradiation begins and to obtain the standard deviations of measurements. Matlab software version R2020b was used to analysed the measurement result.

Equation 1 was used to perform the dose comparison between the measured and planned doses with a criterion of $\pm 3\%$. Additionally, gamma index analysis was carried out using dose difference (DD) and distance to agreement (DTA) 3% /3 mm with gamma index passing rate of 90% [16].

$$\text{Discrepancy (\%)} = \frac{\text{Dose}_{\text{Calculated}} - \text{Dose}_{\text{Measured}}}{\text{Dose}_{\text{Measured}}} \times 100\% \quad (1)$$

Dose volume histogram derived from the planning was also compared with the measured DVH generated from the measurement using Delta⁴ phantom⁺. The DVH is evaluated by $D_{95\%}$ of the target and the maximum dose (D_{Max}) on the OAR. Homogeneity index (HI) was also considered for the DVH evaluation, and the value was determined using Equation (2).

$$\text{HI} = \frac{D_{2\%} - D_{98\%}}{D_{50\%}} \quad (2)$$

Where $D_{2\%}$ is the dose value at 2% planning target volume (PTV), $D_{98\%}$ is the dose value at 98% target volume (PTV), $D_{50\%}$ is the dose value at 50% of the planning target volume (PTV). Homogeneity index represents the uniformity of the absorbed-dose distribution, and an HI value of zero indicates that the absorbed distribution is almost homogeneous [17].

Results

Point Dose Measurement

The results of point dose measurement in superior-inferior motion between the planned and measured doses are shown in Table 1 and Figure 3. Error bars at each point dose generated from TPS indicate the acceptable dose tolerance with the criterion of $\pm 3\%$. However, error bars at each point of the measured dose indicate the standard deviation of the dose measurement. Overall, the measured point dose was lower than the planned point dose.

Table 1. Comparison of point dose measurements and planning dose for all motion variations with 50 mm, and 25 mm field width.

Field width (mm)	Amplitude (mm)	Period (s)	Measured dose (cGy)	Planned dose (cGy)	Discrepancy (%)
25	0	0	214,6	212,16	1,150
	2	4	205,10 ± 2,29	209	-1,864
	4		204,50 ± 0,29	208,68	-2,004
	6		203,89 ± 0,76	207,64	-1,805
	8		204,50 ± 0,57	207,52	-1,456
	10	203,69 ± 0,49	207,32	-1,751	
	2	6	203,89 ± 0,29	209	-2,444
	4		200,05 ± 0,94	208,68	-4,134
	6		180,65 ± 19	207,64	-12,997
	8		185,50 ± 8,44	207,52	-10,610
10	177,42 ± 4,46		207,32	-14,421	
10	0		0	210,36	210,00
50	2	4	203,41 ± 0,2	206,96	-1,714
	4		204,62 ± 0,67	208,72	-1,962
	6		204,22 ± 1,66	208,32	-1,968
	8		203,82 ± 0,91	207,84	-1,936
	10	202,20 ± 0,97	207,88	-2,731	
	2	6	203,89 ± 1,62	206,96	-2,688
	4		200,05 ± 0,25	208,72	-2,156
	6		180,65 ± 1,66	208,32	-1,677
	8		185,50 ± 7,97	207,84	-1,254
	10		177,42 ± 6,4	207,88	-1,661

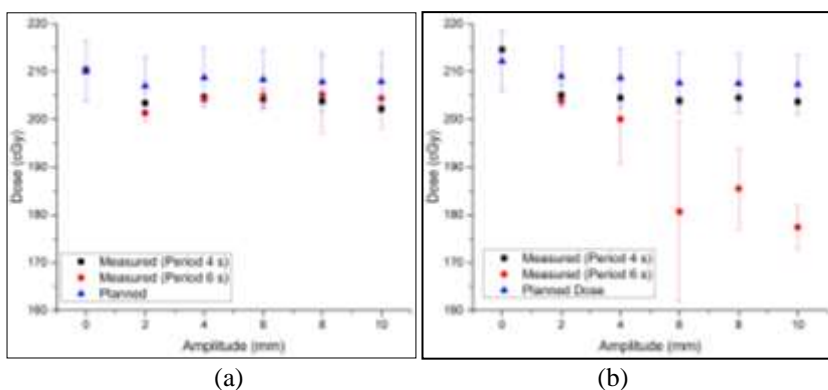


Figure 3. Point dose measurements results for all motion variations with a. 50 mm, and b. 25 mm field width.

The maximum discrepancy was -14.42%, attained when the phantom movement was set at the amplitude of 10 mm and the period of 6 s on the planning parameter with 25 mm jaw width. The standard deviation (SD) of the measurement results represent the uncertainty of the detector position against the phantom motion. As seen in Figure 3, the largest SD is found with a 25-mm jaw width and the phantom movement set at a period of 6 s.

Gamma Index

Global gamma index analysis of the measurement results with varied amplitudes, periods, and jaw widths is presented in Figure 4. It is shown that the larger field width, the smaller amplitude, and period could increase the passing gamma index value.

Looking at the measurement results with a 50-mm jaw field width, the value of the gamma index showed a better passing rate as compared to the measurement results when using a smaller field width. In contrast, using the jaw field width of 25 mm with the motion amplitude of 10 mm and the period of 6 s yielded the lowest passing rate of $61.2 \pm 1.23\%$.

The variation of amplitude and period in the phantom motion caused a substantial effect on the gamma index passing rate when the machine parameter was determined at 25 mm field width. As revealed in the measurement results, using a 25-mm field width, the passing rate with the criterion of more than 90% was only on the expanded target with the amplitudes of 2 mm and 4 mm set at a period of 4 s and the magnitude of 2 mm set at a period of 6 s. Based on the overall results, the passing rate result for the periods of 4 s and 6 s

at the smaller field width indicated a greater uncertainty between the measured dose and the planned dose.

Dose Volume Histogram (DVH)

Homogeneity index, as illustrated in Figure 5, demonstrated the level of dose homogeneity in the target organ. The ideal value of HI is 0, showing homogeneous dose distribution in the target organ. As noted in the measurement result in Figure 5, an increase in the phantom motion amplitude resulted in a non-homogeneous dose distribution in the target organ, which can be minimized with the selection of a larger field width to account for the movement effect on the target.

$D_{95\%}$ between the planned and measured doses in target structures and D_{Max} in OAR structures for original and expanded structures are described in Table 2. $D_{95\%}$ represents the minimum dose received in the target [18]. Looking at the overall measurement results, the effect of target motion can lead to the reduction of dose coverage at 95% target volume. This could be more pronounced with the use of a smaller field width, a higher amplitude, and a greater motion period of the target organ. As observed in all the measurements, the effect of movement on the target can reduce coverage $D_{95\%}$ of the dose distribution in the expanded target structure. The biggest dose difference at $D_{95\%}$ occurs when using a jaw width of 25 mm, and the largest amplitude movement at a period of 6 s is around -0.271 Gy.

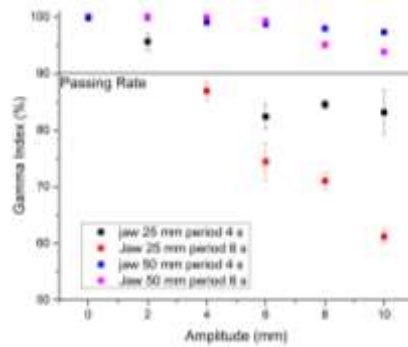


Fig 4. Gamma index analysis for all motion variations.

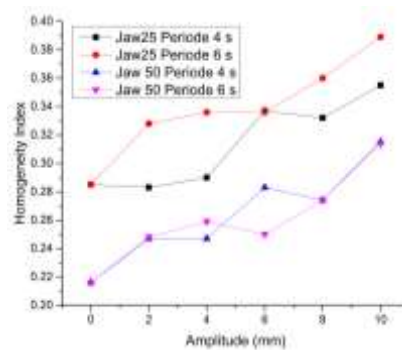


Figure 5. The HI values for all motion variations

Table 2. Dose difference analysis between measurement and planning data for $D_{95\%}$ in target structure and D_{Max} in OAR structure.

Amplitude (mm)	Period (s)	$D_{95\%}$ Structure of Target (Gy)		D_{Max} structure of OAR (Gy)	
		25 mm Field Width	50 mm Field Width	25 mm Field Width	50 mm Field Width
0	0	-0.098	-0.081	0.157	0.082
2		-0.143	-0.101	0.091	0.248
4		-0.143	-0.122	0.102	0.11
6	4	-0.114	-0.092	0.191	0.249
8		-0.091	-0.071	0.195	0.27
10		-0.09	-0.122	0.283	0.327
2	6	-0.133	-0.081	0.157	0.082
4		-0.143	-0.122	0.097	0.254
6		-0.173	-0.081	0.107	0.155
8		-0.154	-0.092	0.193	0.27
10		-0.271	-0.061	0.205	0.236

In terms of the OAR, the measured dose received by OAR was predominantly higher than the planned dose in all the measurement setups. A higher amplitude will result in a more powerful increase in the maximum dose received by the expanded OAR structure. The phantom motion amplitude of 10 mm and a period of 4 s produced the largest difference of the maximum dose at expanded OAR by 0.327 Gy at the field width of 50 mm.

Discussion

The dosimetric impact of longitudinal motion on dose distribution in helical tomotherapy was evaluated by varying some parameters of phantom movement in both original and expanded structures. The results indicated that the target motion could affect the dose distribution at the target and the adjacent OAR. This study was a phantom-based measurement, and the structures were delineated in the C-shape for the target structure according to the AAPM TG-119 report.

Point dose measurement using an AISL detector showed the tendency of the measured dose to have a lower value than the planned dose. The decrease in the dose received by the detector was due to the partial volume of the detector receiving the dose during irradiation. Target motion was not synchronized with MLC, which means that the correlation of tumor motion as a consequence of the patient's respiration and the motion of MLC is independent. The interplay effect phenomenon could generate undesired dosimetry effect as of under dosage [19], and irregular respiratory motion can lead to decreased dose in target volume by $4.1\% \pm 1.7\%$ in the amplitude of 10 mm and by $9.6\% \pm 1.7\%$ in the amplitude of 20 mm [20].

The proper selection of field width in the treatment parameter for the moving target is very important. Based on the dose verification result using the ionization chamber detector, the amount of phantom motion could affect the amount of radiation passing through the ionizing chamber volume. In this study, the average dose for the target volume derived from the treatment planning system was determined by considering the phantom motion amplitude to expand the target volume and the amount of the amplitude applied to the phantom setup. However, using the smaller field width still produced a considerable difference in dose distribution between the measured and planning doses.

The remarkable impact of phantom motion on the dose distribution variation between the measured and planned doses was seen at the phantom amplitude of 6 mm using a 25-mm field width (Figure 3). This result confirmed with the findings of Kim et al. [13], who noted a the bigger dose discrepancy resulting from a smaller jaw field width. In the treatment planning system, the original active volume of detector was 4 mm with a motion amplitude of 6 mm to expand the original active volume of detector contour of the target by 6 mm in both superior and inferior target contours. The consequence of the total length of the expanded contour was 16 mm. The dose prescription of 2 Gy per fraction was delivered to the expanded contour. The reference

point dose was calculated using simulated expanded structure at the TPS when using a 25-mm jaw field width with a motion amplitude of about 6 mm. The impact in the distance between the superior and inferior edges of the expanded contour was slightly closer to the edge limit of the projected field width (at the penumbra region). Once the phantom with the AISL detector inside was moved in the longitudinal direction, the 25-mm jaw field width could not cover the whole volume of the detector as contoured and calculated in the TomoPlan. Subsequently, the predicted dose distribution differed from the measured dose distribution. At greater motion amplitudes (i.e., 8 mm and 10 mm), the dose rippling effect occurred at center of the structure, and it could increase the average dose in the target volume structure. Furthermore, the target motion and the time of radiation were independent variables and the jaws were static corresponding to the phantom movement in a longitudinal direction. The implementation of the dynamic jaw and motion management, additionally, could improve the dose coverage in the target's motion.

The results of gamma index analysis with the passing rate criterion of more than 90% showed that the target motion affected the gamma passing rate results. As seen in Figure 4, the gamma passing rate was lower if the phantom motion amplitude increased. The increasing phantom magnitude on the moving platform could add the penumbra dose at the superior and inferior edges of the target volume because the radiation area in the longitudinal direction became longer and resulted in the dose artifact as a consequence of target motion [7]. However, using a larger field width for the expanded target with the motion amplitude of 10 mm and the motion periods of 4 s and 6 s could reduce the dose variation due to dose rippling [11]. Dose rippling is a series of periodic dose peaks and valleys observed along the direction of table motion due to the non-synchronization between the table motion and the target's motion. Using a larger field width, in the same target size, could produce less amount of helical beam junction compared to the smaller field width employed, which could improve the passing rate of gamma index.

Gamma passing rate was not truly influenced if the movement amplitude was up to 10 mm, the period was 4 and 6 s, and the jaw width was 50 mm, as shown in Figure 4. Moreover, all the analyzed data met the acceptable limit when the value of gamma passing rate was more than 90%. These results are in line with the findings of Yang [8], presenting that the target motion with the maximum amplitude of 10 mm and the period of 4 s had a passing rate of more than 90% and fulfilled the DD/DTA criterion of 3%/3 mm. However, when using a 25-mm jaw width, the increasing phantom movement period considerably influenced the gamma passing rate. This finding is in line with the study reported by Klein et al. (2013) [11], showing that 25% dose rippling could be produced corresponding to the target motion with a period of 10 s.

The increasing motion amplitude of the target during irradiation caused the dose distribution in the target

volume to become more non-homogeneous, as seen in Figure 5. The target contour shape, used in this study, could probably influence the dose homogeneity as the complexity of the target contour could contribute to the non-synchronized effect of MLC pertaining to the target motion. For example, MLC properties and beam fluences derived from the TPS with the static field width, once delivered to the target's motion, the dose distribution might differ due to the fact that beam modulation and MLC properties do not account for the target's motion during irradiation.

The use of different periods with the same amplitude impacted the difference in the rate of movement in each variation. Based on the measurement results with the variation of the phantom motion period, increased motion period could produce a prominent discrepancy and generated artifact to dose distribution [21]. A wider scope of artifacts occurs due to the non-synchronized opening of MLC in IMRT on the target motion. Moreover, the use of a bigger jaw imposed smaller effects on helical tomotherapy dose distribution for the moving target, since the presence of bigger penumbra provided an additional dose to the target edge when the target moved [7].

A higher motion amplitude would increase the dose received by OAR structures, and the dose difference between the measured and planned doses yielded an interesting result by using the larger field width. A bigger difference in dose occurs in both superior and inferior of OAR structure. This could happen through the effect of dose rounding. Dose rounding effect due to the use of a larger field width has a larger area of penumbra, and the introduction of target motion could produce a considerable dose variation between the planned and measured doses. Additionally, target's motion could contribute to the dose artefact in the OAR structure [11]. Looking at the planning results, the dose in the OAR structure was predominantly a low dose. The dose rounding effect caused the superior and inferior edges of expanded OAR structures receive a higher radiation intensity compared to the middle section. The selection of jaw field width, therefore, is crucial to create a better planning quality in the case of target motion treated in helical Tomotherapy.

Conclusion

In this study, point dose measurement, gamma index, HI, and dose difference were investigated using Cheese and Delta4+ phantoms on a moving platform. The phantom amplitude and period affected the dose distribution produced by tomotherapy system on IMRT techniques based on AAPM TG-119. The target's motion could induce dose discrepancies due to dose rippling, dose rounding, and non-synchronized opening of MLC. The selection of jaw field width becomes crucial for IMRT techniques since the dose discrepancy between the planned and measured doses showed an excellent result for gamma index and dose coverage while using a larger field width. Furthermore, point dose

measurements yielded smaller values for all variation movements compared to the TPS.

Acknowledgment

This work was supported by PIT-9 research grant No: NKB-0034/UN2.R3/HKP.05.0012019 funded by Universitas Indonesia.

References

1. Mackie T R, Holmes T, Swerdloff S, Reckwerdt P, Deasy J O, Yang J, et al. Tomotherapy: a new concept for the delivery of dynamic conformal radiotherapy. *Med. Phys.* 1993; 20:1709-19.
2. Keall PJ, Mageras GS, Balter JM, Emery RS, Forster KM, Jiang SB, et al. The management of respiratory motion in radiation oncology report of AAPM Task Group 76. *Med. phys.* 2006;33(10):3874-900.
3. Ezzell GA, Burmeister JW, Dogan N, LoSasso TJ, Mechalakos JG, Mihailidis D, et al. IMRT commissioning: multiple institution planning and dosimetry comparisons, a report from AAPM Task Group 119. *Med Phys.* 2009;36(11): 5359-73.
4. Bortfeld T, Jiang SB, Rietzel E. Effects of Motion on the Total Dose Distribution. *Seminars in Radiation Oncology.* 2004;14(1):41-51.
5. Stevens CW, Munden RF, Forster KM, Kelly JF, Liao Z, Starkschall G, et al. Respiratory-Driven Lung Tumor Motion Is Independent Of Tumor Size , Tumor Location , And Pulmonary Function . *Int J Radiat Oncol Biol Phys.* 2001;51(1): 62-8.
6. Plathow C, Ley S, Fink C, Puderbach M, Hosch W, Schmähl A, et al. Analysis of intrathoracic tumor mobility during whole breathing cycle by dynamic MRI. *Int J Radiat Oncol Biol Phys.* 2004;59(4):952-9.
7. Kanagaki B, Read PW, Molloy JA, Lerner JM, Sheng K. A motion phantom study on helical Tomotherapy: The dosimetric impacts of delivery technique and motion. *Phys Med Biol.* 2007;52(1):243-55.
8. Yang JN, Mackie TR, Reckwerdt P, Deasy JO, Thomadsen BR. An investigation of Tomotherapy beam delivery. *Med Phys.* 1997;24(3):425-36.
9. Yu CX, Jaffray DA, Wong JW. The effects of intrafraction organ motion on the delivery of dynamic intensity modulation. *Phys Med Biol.* 1998;43(1):91-104.
10. Kissick M W, Boswell S A, Jeraj R, Mackie T R. Confirmation, refinement, and extension of a study inintrafraction motion interplay with sliding jaw motion. *Med. Phys.* 2005; 32(7Part1): 2346-50.
11. Klein M, Gaede S, Yartsev S. A study of longitudinal tumor motion in helical Tomotherapy using a cylindrical phantom. *J Appl Clin Med Phys.* 2013;14(2):52-61.
12. Park SH, Choi J, Kim J, Ahn S, Kim MJ, Lee H, et al. Impact of the Respiratory Motion and Longitudinal Profile on Helical Tomotherapy. *PMP.* 2018;29(1):1-7.
13. Kim B, Chen J, Kron T, Battista J. Motion-induced dose artifacts in helical Tomotherapy. *Phys Med Biol.* 2009;54(19):5707-34.

14. Langen KM, Papanikolaou N, Balog J, Crilly R, Followill D, Goddu SM, et al. QA for helical Tomotherapy: Report of the AAPM Task Group 148. *Medical Physics*. 2010;37(9): 4817-453.
15. Bedford JL, Lee YK, Wai P, South CP, Warrington AP. Evaluation of the Delta4phantom for IMRT and VMAT verification. *Phys. Med. Biol.*. 2009;54(9): N167.
16. Low DA, Moran JM, Dempsey JF, Dong L, Oldham M. Dosimetry tools and techniques for IMRT. *Med phys*. 2011;38(3): 1313-38.
17. Gregoire V. ICRU, Report 83: Prescribing, Recording, and Reporting Photon-Beam Intensity-Modulated Radiation Therapy (IMRT). *Journal of the ICRU*. 2010;10(1).
18. Allisy A. ICRU, report 50. Prescribing, Recording, and Reporting Photon-Beam Photon Beam Therapy. ICRU Publ Bethesda MD.1993.
19. Larsson T. Accuracy of MLC-tracking for inversely optimized arc therapy treatments of varying complexity for two MLCs [dissertation]. Lund: Lund University. 2010.
20. Mutaf YD, Scicutella CJ, Michalski D, Fallon K, Brandner ED, Bednarz G, et al. A Simulation Study of Irregular Respiratory Motion and its Dosimetric Impact on Lung Tumors. *Phys. Med. Biol.* 2011;56(3): 845-59.
21. Chaudhari SR, Goddu SM, Rangaraj D, Pechenaya OL, Lu W, Kintzel E, et al. Dosimetric variances anticipated from breathing-induced tumor motion during Tomotherapy treatment delivery. *Phys. Med. Biol.* 2009;54(8): 2541-55.